Viterbi-Viterbi Carrier Phase Estimation for Multi-Ring M-APSK With Wiener Carrier Phase Noise and Its Performance

Qian Wang , *Member, IEEE*, Wenqiang Ma, Li Ping Qian , *Senior Member, IEEE*, Xinwei Du , *Member, IEEE*, Changyuan Yu , *Senior Member, IEEE*, and Pooi-Yuen Kam , *Life Fellow, IEEE*

Abstract—High-order modulations are currently widely used in optical communications to increase the data rate. However, due to the existence of laser phase noise, the performance of high-order modulated systems will be greatly degraded. Therefore, phase estimation (PE) methods and laser linewidth tolerance analysis are particularly important in practice. In this paper, we first propose a common refined Viterbi-Viterbi carrier phase estimator for multi-ring M-ary amplitude phase-shift keying (M-APSK) with Wiener phase noise. The design is based on the linear minimum mean square error (LMMSE) criterion to optimize the weight coefficients with respect to the statistics of Wiener phase noise and additive, white, Gaussian noise. For simple implementation, approximate ring-detection-based and average-energy-based LMMSE estimators are further derived for multi-ring modulations. The laser linewidth tolerance in Wiener phase noise is analyzed thoroughly compared to the popular PE methods, e.g., decision-aided maximum likelihood and QPSK partitioning. Numerical results show in detail the receiver sensitivity penalties as a function of the estimation memory length, and verify that the proposed estimators do not suffer from the block length effect and perform much better at high signal-to-noise ratio (SNR). They are suitable for coherent demodulation of a multi-ring signal constellation in high SNR or fast-varying phase noise.

Index Terms—M-ary amplitude phase-shift keying, wiener phase noise, linear minimum mean square error, carrier phase estimation, laser linewidth tolerance.

I. INTRODUCTION

WITH the rapid development of both wireless and optical communication systems, the demand for data transmission rate is growing fast. High-order modulation formats, such as M-ary phase-shift keying (PSK), quadrature amplitude modulation (QAM) and amplitude phase-shift keying (APSK), have been considered positively to improve the spectrum efficiency [1], [2], [3]. However, phase noise due to the imperfect local oscillators (LO) is one major limiting factor to degrade the coherent performance, especially for high-order modulated transmission [4]. Specifically in coherent optical systems, analyzing the laser phase noise effect on the transmission efficiency is very important, and this thus brings a lot of analytical investigations [5], [6]. For example, the laser phase noise tolerance of high-order probabilistically shaped and uniformly shaped QAM signals is analyzed in [7]. Reference [8] considered the laser linewidth tolerance for the set-partitioning QAM after carrier phase recovery in phase noise.

Considering the presence of phase noise, the compensation for the unknown carrier phase based on phase estimation (PE) before data detection is indispensable [9]. To overcome the disadvantages of the optical phase-locked loop, several digital signal processing-based PE algorithms have been investigated recently. For example, [10] proposed the explicit structures of phase based, joint maximum likelihood (ML)/maximum a posteriori (MAP) estimation of unknown single-sinusoid angle parameters affected by time-varying phase noise. A novel PE scheme based on local convex optimization for multi-level modulations was derived in [11], which has a good flexibility and achieves a balance between algorithm cost and estimation accuracy. Reference [12] considered the problem of phase reference estimation with noise, and proposed a machine learning approach based on clustering algorithms to mitigate the negative effects of phase noise. By further optimizing the Mth-power estimator in Wiener phase noise, [13] derived a refined linear minimum mean square error (LMMSE) phase estimator for M-PSK, which can be efficiently implemented in real time. The proposed LMMSE estimator has better performance and does not suffer from the block length effect, compared to many popular methods, e.g., decision aided (DA) ML PE in [14]. Note that most existing algorithms derived do not consider the random
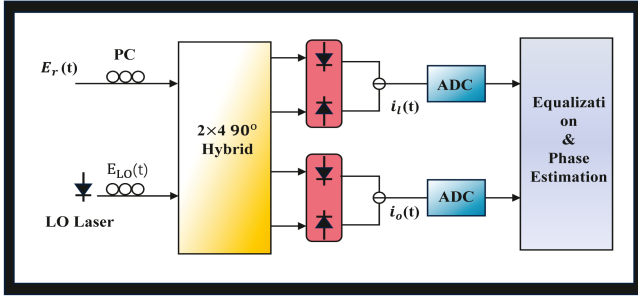
Fig. 1. Digital coherent receiver. PC: polarization-controller. ADC: analog-to-digital converters.

Fig. 2. Multi-ring constellations: Star-8QAM and 16APSK(8,8).

process of Wiener phase noise, or cannot be simply generalized to high-order multi-ring modulations.

In this paper, we consider the refinement of Viterbi-Viterbi (VV) carrier phase estimation for multi-ring M-APSK and analyze its laser linewidth tolerance in Wiener phase noise. The design is based on the LMMSE criterion to optimize the weight coefficients with respect to the statistics of Wiener phase noise and additive, white, Gaussian noise (AWGN), which is similar to the derivation of the refined LMMSE estimator for single-ring M-PSK with Wiener phase noise in [13]. For simple implementation, two simplified estimation criteria including ring-detection-based and average-energy-based estimators are further derived for multi-ring M-APSK. The inverse mean square error (IMSE) performance is analyzed in detail for the three proposed LMMSE estimators by simulations. It is shown that the common refined VV estimator performs much better than the simplified ones in low or moderate signal-to-noise ratio (SNR) range, which is yet at the cost of high complexity of matrix inversion. In comparison with other popular methods, e.g., DA ML and QPSK partitioning, the receiver sensitivity penalties are also given for different modulation formats including 16QAM. It is to verify that the proposed estimators perform much better at high SNR and the estimation accuracy is immune to the block length effect.

The rest of this paper is structured as follows. The signal model is presented in Section II. The common refined LMMSE estimator and the simplified ones for multi-ring M-APSK are derived in Section III. The numerical results are given in Section IV. The last section concludes the paper.

II. SIGNAL MODEL

As shown in Fig. 1, the received signal is first combined with an LO laser in a 2×4 90° optical hybrid, then the output signals are detected by the in-phase and quadrature-phase signal balanced detectors. After sampling by a high-speed analog-to-digital converter, the signals will be processed by digital equalization and phase estimation. We assume that the polarization controller can make the polarization perfectly matched, and the inter-symbol interference caused by the dispersion is completely compensated by the digital equalization. Thus, we only consider the effect of AWGN and laser phase noise here. In this case, the received signal model over the kth symbol interval is given
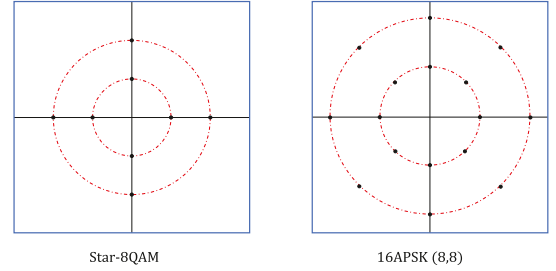
by [13],

$$
\begin{aligned}
r(k) &= m(k)e^{j\theta(k)} + n(k) \\
&= |r(k)|e^{j\angle r(k)} = |r(k)|e^{j[\phi_i(k)+\theta(k)+\epsilon(k)]}.
\end{aligned} \tag{1}
$$

Here, $|r(k)|$ and $\angle r(k)$ represent the amplitude and phase of the received signal $r(k)$, respectively. Term $m(k)$ is the kth transmitted signal chosen from the M equally likely signal points $\{S_i = A_i e^{j\phi_i}, \ i = 0, 1, \ldots, M-1\}$, in which A_i and ϕ_i, respectively, represent the amplitude and phase of each modulated signal. Term $n(k)$ stands for the AWGN, which is a Gaussian random variable with mean zero and variance N_0. And $\theta(k)$ stands for the phase noise, which is modeled as a Wiener process, i.e., $\theta(k) = \theta(k-1) + v(k)$ [13]. Term $\{v(k)\}$ is a sequence of independent, identically distributed Gaussian random variables with mean zero and variance $\sigma_p^2 = 2\pi\Delta v T_s$, where T_s and Δv represent the symbol duration and the total 3-dB laser linewidth of the transmitter and local oscillator lasers, respectively. Term $\epsilon(k)$ denotes the additive, observation phase noise (AOPN) due to the AWGN, which is approximately Gaussian distributed with mean zero and variance $\sigma_\epsilon^2(k) = \frac{N_0}{2|r(k)|A_i}$ in high SNR [9].

For general M-APSK, the signal set is $\{S = a_k e^{j(\frac{2\pi i}{l_k}+\psi_k)}$: $1 \le k \le N$, $0 \le i \le l_k - 1\}$, where N is the number of signal rings, a_k, l_k and ψ_k denote the radius, the number of points and the relative phase shift corresponding to the kth ring, respectively [4]. We have $\sum_{k=1}^{N} l_k = M$, and the radii are assumed to be ordered such that $a_1 < \cdots < a_N$. The average energy constraint is thus $\sum_{k=1}^{N} l_k a_k^2 = M E_s$, where E_s denotes the average energy per symbol. We also define the vector $\boldsymbol{l} \equiv (l_1, \ldots, l_N)$ and use the notation MAPSK-$\boldsymbol{l}$ for an M-APSK constellation with N rings and l_k signal points on the kth ring, e.g., 16APSK(8,8). Note that for a specific M-APSK with given N, placing almost the same number of signal points on each ring leads to the minimum error floor due to the phase noise, which has been verified in our earlier work [4]. Thus, we consider star-8QAM and 16APSK(8,8) as examples for numerical illustration here, as shown in Fig. 2.

In the following, we will derive a common refined VV carrier phase estimator for any multi-ring M-APSK. Note that there are not that many techniques available at the moment for carrier recovery of multi-ring constellations. This work here provides

the non-decision aided carrier phase estimator for M-APSK constellations in general that are circular and consisting of multiple rings in which the signal points are uniformly distributed.

III. REFINED LMMSE PE FOR MULTI-RING M-APSK

This section will first introduce the general VV phase estimator based on the LMMSE criterion for multi-ring M-APSK with Wiener phase noise. Then two simplified implementations including both ring-detection based estimator and average-energy based estimator are given in detail.

Based on our previous work in [13] on the refined LMMSE PE for M-PSK in Wiener phase noise, this work also considers to estimate each M-APSK symbol using an estimation window of size $2L+1$, including the current symbol and its earlier and later L symbols. Here, L is the memory length. By referring to the conventional Mth-power carrier phase estimation, raising the received symbol to the Mth-power and taking the normalization will remove the phase modulation, which thus gives

$$y_M(k) = \left[\frac{r(k)}{|r(k)|} \right]^M = \left[e^{j[\phi(k)+\theta(k)+\epsilon(k)]} \right]^M$$
$$= e^{j[M[\theta(k)+\epsilon(k)]]}. \quad (2)$$

It is worth emphasizing that the M in the Mth power here is the least common multiple of $(l_1, \ldots, l_N)$ considering all signal rings, instead of the modulation order. That is, given 16APSK(8,8) for example, the M in the Mth power is $M = 8$. In this way, $M\phi(k) = 2\pi$ can be removed. Thus, based on the observations within the symmetrical window, i.e., $\{y_M(l)\}_{l=k-L}^{k+L}$, the phase estimate $\hat{\theta}(k)$ can be obtained using this refined Mth-power estimator. Here, we will give the derivation for M-APSK with the consideration of both AWGN and Wiener phase noise.

With the phasor at the kth time interval denoted as $V_M(k) = e^{jM\theta(k)}$, the estimated phasor using the refined method is similarly given by [13, eq. (23)]

$$\hat{V}_M(k) = \sum_{l=k-L}^{k+L} F(|r(l)|)y_M(l) = \mathbf{w}^H \mathbf{y_M}(k) \quad (3)$$

where $\mathbf{y_M}(k) = [y_M(k-L), \ldots, y_M(k+L)]^T$ represents the observation vector for the kth time interval, and $\mathbf{w} = [F(|r(k-L)|), \ldots, F(|r(k+L)|)]^H$ denotes the complex weight coefficients, which can be chosen to optimize the estimation performance. Here, superscripts T denotes the transpose and H denotes the Hermitian transpose. Previously, the optimal nonlinearity $F(|r(l)|)$ was discussed with AWGN only. For example, the optimal nonlinearity of $F(|r(l)|) = |r(l)|^2$ was verified in [13] for M-PSK. Here, with the consideration of both AWGN and linear phase noise, the optimal $F(|r(l)|)$ can be derived explicitly based on the LMMSE criterion. Specifically, the estimation error can be expressed as $e(k) = V_M(k) - \hat{V}_M(k)$, and by minimizing the mean squared error $E[|e(k)^2|]$, the optimal weight coefficient $\mathbf{w}_o$ can be obtained as [13, eq.(27)]

$$\mathbf{w}_o = \mathbf{R}^{-1}\mathbf{p}, \quad (4)$$

where $\mathbf{p}$ is the $(2L+1) \times 1$ cross-correlation vector, and $\mathbf{R}$ is the $(2L+1) \times (2L+1)$ auto-correlation matrix. The lth term of $\mathbf{p}$ is

given by

$$p_l = e^{-\frac{1}{2}M^2\left(|L-l+1|\sigma_p^2+\sigma_\epsilon^2(k-L+l-1)\right)}, \quad (5)$$

and the (x, y) element of $\mathbf{R}$ is given by

$$R(x,y) = e^{-\frac{1}{2}M^2\left[(|x-y|)\sigma_p^2+\sigma_\epsilon^2(k-L+x-1)+\sigma_\epsilon^2(k-L+y-1)\right]}, \quad (6)$$

and the AOPN variance $\sigma_\epsilon^2(k)$ therein is given as

$$\sigma_\epsilon^2(k) \approx \frac{N_0}{2|r(k)|^2}. \quad (7)$$

This approximation is because we have $|r(k)| \approx A_i$ in high SNR for most times [9], and this form does not require the priori information on the transmitted amplitude A_i. The detailed derivation is similar to the process in [13, Appendix A], which is thus avoided here. We will verify the accuracy of this refined LMMSE estimator (3) for multi-ring M-APSK by simulations later. Note that both $\mathbf{p}$ and $\mathbf{R}$ are time-varying due to the fluctuation of the received signal amplitude $|r(k)|$ in the AOPN variance $\sigma_\epsilon^2(k)$. Thus, we consider two simplified implementations in the following, which are computationally more efficient and more suitable in practice.

For the first simplification, the main idea is to treat the multi-ring M-APSK as one single-averaged-ring M-PSK. In this way, estimating multi-ring modulated phase can be approximated to estimating one single-averaged-ring modulated phase. Therefore, in the estimation process, we first determine which ring the received signal in the estimation window belongs to, and then using the mean of all received a_i for the weight calculation after ring detection. The ring detection rule used here is given as [9, eq.(12)]

$$|r(k)| \underset{\widehat{A}=a_{i+1}}{\overset{\widehat{A}=a_i}{\lessgtr}} r_{th} = \frac{a_i + a_{i+1}}{2}, \quad (8)$$

where a_i and a_{i+1} represent the radii of the ith and $(i+1)$th rings, respectively, and $\widehat{A}$ denotes the ring decision of the received signal. Note that for the special case of M-APSK, e.g., 16APSK(8,8) where each ring has the same number of points with the same phase values, our earlier work in [9] has verified that the two-step detector that first determines the ring and then the phase is equivalent to the approximate optimum detector through the whole SNR region. This implies that the ring detection error induced by (8) can be ignored, especially for high SNR. After ring detection, we can calculate the mean of all received a_i in the estimation window, denoted as $\bar{a}_i$ for the estimation weight calculation. That is, we average the radii obtained by the detection rule throughout the received window to replace $|r(k)|$ in calculating $\sigma_\epsilon^2(k)$. In this way, the corresponding AOPN $\sigma_\epsilon^2(k)$ can be approximated as

$$\sigma_\epsilon^2(k) \approx \frac{N_0}{2\bar{a}_i^2}. \quad (9)$$

And thus, we have the calculation of (5) and (6) simplified as

$$p_l = e^{-\frac{1}{2}M^2\left(|L-l+1|\sigma_p^2+\frac{N_0}{2\bar{a}_i^2}\right)}, \quad (10)$$

and

$$R(x,y) = e^{-\frac{1}{2}M^2\left[(|x-y|)\sigma_p^2 + 2\frac{N_0}{2\bar{a}_i^2}\right]}. \tag{11}$$

The estimated phasor values $\hat{V}(k)$ will be obtained based on (8)–(11). This process is denoted as the ring-detection based LMMSE estimator for M-APSK.

In addition to the simplified ring detection-based estimator, we further consider another approximate implementation using the average energy per symbol. We assume that the received amplitude $|r(k)|$ approaches closely to $\sqrt{E_s}$ in high SNR. Thus, the AOPN variance $\sigma_\epsilon^2(k)$ can be further approximated as a constant

$$\sigma_\epsilon^2 \approx \frac{N_0}{2E_s}, \tag{12}$$

where E_s/N_0 represents the average SNR per symbol. We define the implementation of (3), (4), (10)–(12) as the average-energy based LMMSE estimator. It is worth noting that the approximate σ_ϵ^2 in (12) makes the calculation of $\mathbf{w}_o$ be performed only once in the entire phase estimation process, which greatly reduces the implementation complexity.

In brief, we first propose the common refined LMMSE PE for multi-ring M-APSK in Wiener phase noise, where the optimal nonlinearity of $F(|r(l)|)$ is also shown as a function of $|r(l)|^2$ due to using the AOPN variance in (7). Then two simple implementations for practical applications are introduced based on the assumption of constant σ_ϵ^2. Obviously, the simplification or the assumption would degrade the estimation accuracy, particularly at low SNR. To verify its feasibility, the performance impairment due to the simplified implementation is evaluated through numerical simulations later. More importantly, the laser linewidth tolerance analysis in Wiener phase noise will be given explicitly, compared to the existing popular PE methods, e.g., DA ML in [14]. Note that the DA ML estimator is statistically optimum in the presence of AWGN and a quasi-static carrier phase process [15], but its application is less common in practice than that of the Mth-power estimator, since the latency issue associated with the need for making symbol decisions before performing the decision-aided phase estimation can cause a serious problem in practical receiver implementations.

IV. NUMERICAL RESULTS

This section analyzes the laser linewidth tolerance of the refined LMMSE PE for multi-ring constellations in Wiener phase noise by Monte Carlo simulations. For comparison, the performance of the well-known DA ML PE on multi-ring APSK and the popular QPSK partitioning method on 16QAM are investigated. The performance comparison between the existing methods and proposed algorithms is conducted in terms of IMSE and SNR penalty. In this paper, the SNR penalty is calculated via simulations and is the value of the difference between required SNRs under the phase noise channel and the pure AWGN channel.

In order to combat the phase ambiguity caused by the Mth-power operation, Genie-aided phase unwrapping given in Table I is used here [13].

TABLE I
GENIE-AIDED PHASE UNWRAPPING

Initialize with $\angle\hat{V}_M(k) = \arg[\hat{V}_M(k)]$;
while $\angle\hat{V}_M(k) - M\theta(k) \geq \pi$
$\quad \angle\hat{V}_M(k) = \angle\hat{V}_M(k) - 2\pi$
end
while $\angle\hat{V}_M(k) - M\theta(k) \leq -\pi$
$\quad \angle\hat{V}_M(k) = \angle\hat{V}_M(k) + 2\pi$
end
$\hat{\theta}(k) = \frac{1}{M}\angle\hat{V}_M(k)$

A. IMSE Comparison for Different Implementations

Here, we consider the IMSE comparison among the common refined estimator and the simplified ones including both ring-detection based and average-energy based estimators. In simulations, the IMSE is defined as

$$IMSE = -10\log_{10}\left[\frac{\sum_{k=1}^{q}[\theta(k) - \hat{\theta}(k)]^2}{q}\right], \tag{13}$$

where q denotes the sample size for each calculation of IMSE. To distinguish the three implementations in the plots, the LMMSE notation is used to represent the common refined LMMSE estimator for short, and the LMMSE-ring and the LMMSE-Es denote the ring-detection based and average-energy based simplified implementations, respectively.

Fig. 3 shows the IMSE performance as a function of the memory length L with the laser linewidth fixed at 1 MHz. We can see that the performance of all the implementations becomes better as SNR increases, and it is not affected by the increase of L, i.e., does not suffer from the block length effect. As Fig. 3(a) and (b) show for Star-8QAM and 16APSK(8,8) in relatively high SNR, e.g., 15 dB and 25 dB, the common refined LMMSE estimator performs the best, and the ring-detection based and the average-energy based methods perform a little worse but very close to each other. For example, when SNR=15 dB, the common refined estimator performs about 1 dB better than other two methods. This is expected since the two simplified algorithms sacrifice performance to reduce the time or computation complexity. But in low SNR, e.g., 5 dB, the estimation performance deteriorates fast for all the methods. Especially for 16APSK(8,8) shown in Fig. 3(b), the performance of the common refined estimator drops to the same level as those of the simplified ones.

We also consider the widely used 16QAM here, which can be viewed as the combination of multiple signal rings. Fig. 3(c) shows that the phenomenon for 16QAM at 5 dB and 15 dB is similar to that of 16APSK(8,8). In comparison, the most interesting finding for 16QAM is that the ring-detection based method performs a little bit better than the common refined one at SNR=25 dB. We infer that this is due to the non-symmetric middle-ring structure and the high detection accuracy in high SNR. Additionally, it is worth noting that with the decrease of SNR, the performance of the two simplified algorithms drops faster. This trend similar to that in Fig. 3(a) and (b) is particularly pronounced in 16QAM. For example, in Fig. 3(c), when SNR=15 dB, the performance gap between the simplified
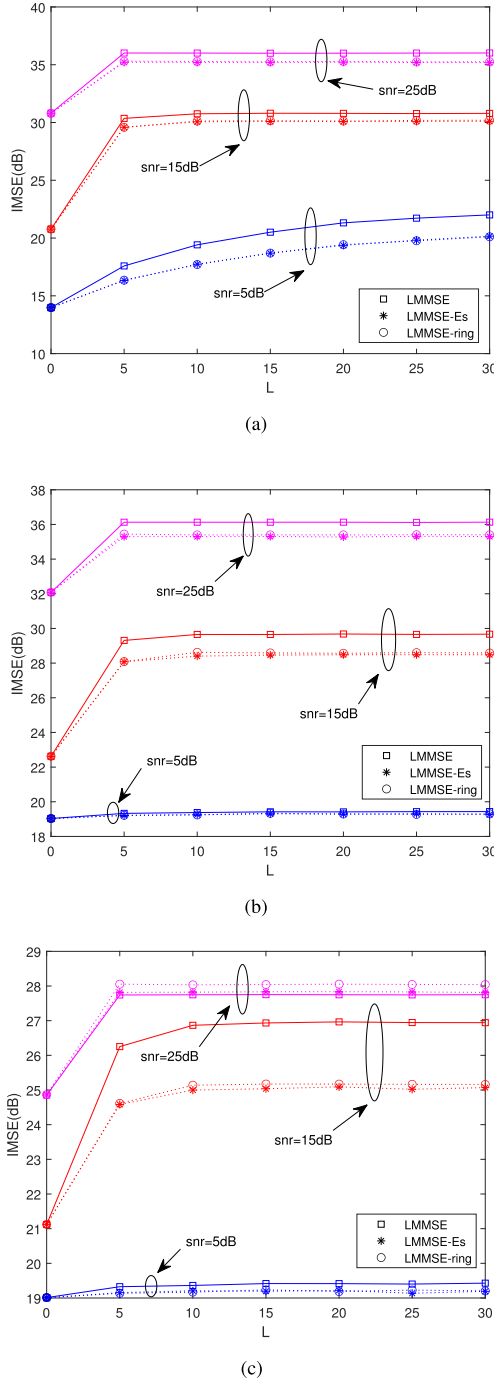
(a)

(b)

(c)

Fig. 3. IMSE performance comparison among three implementations for (a) Star-8QAM, (b) 16APSK(8,8), and (c) 16QAM. Bit rate at 40 Gb/s.

algorithms and the common refined LMMSE algorithm is about 2 dB. When the SNR drops to 5 dB, the performance gain of the common refined LMMSE algorithm decays to be very tiny.

B. Receiver Sensitivity Analysis for Different Modulations

All the three implementations are considered here, and the minimum Euclidean distance detection rule is used after phase estimation. The range of laser linewidths for various modulated

TABLE II
SNR REQUIRED TO ACHIEVE BER$=10^{-2}$ FOR DIFFERENT MODULATION FORMATS

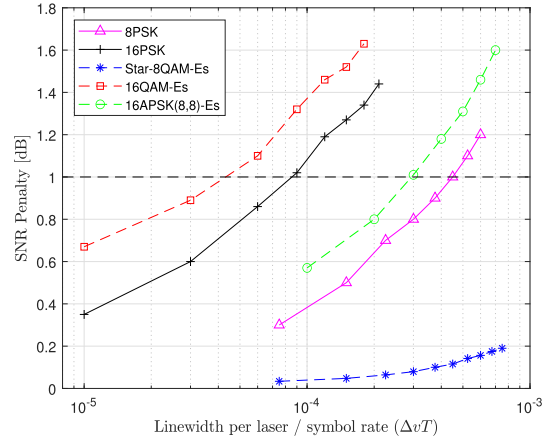| Modulation format	Star-8QAM	16QAM	16APSK(8,8)
Laser linewidth range	0-40 MHz	0-6 MHz	0-4 MHz
SNR range (LMMSE)	9.1-9.3 dB	9.3-9.9 dB	9.0-10.2 dB
SNR range (LMMSE-Es)	9.1-9.6 dB	9.2-10.6 dB	9.3-10.3 dB
SNR range (LMMSE-ring)	9.1-9.6 dB	9.2-10.6 dB	9.3-10.3 dB

Fig. 4. Receiver sensitivity penalties at BER$=10^{-2}$ versus linewidth per laser/symbol rate using average-energy based method. Bit rate at 40 Gb/s.

formats and the corresponding required SNR values are shown in Table II. We can see that the laser linewidth tolerance of star-8QAM is much better than 16-ary formats, which is expected due to the lower sensitivity to phase noise. Moreover, the SNR required for the common refined LMMSE estimator to reach BER$=10^{-2}$ is always the lowest. While the SNR required for the average-energy based method is generally the same as the ring-detection based method. Considering the lower complexity, the average-energy based method will be used in subsequent simulations to analyze the receiver sensitivities for different modulations at BER$=10^{-2}$.

Fig. 4 shows the receiver sensitivity penalty comparison at BER$=10^{-2}$ for different modulations, based on the average-energy based LMMSE method. Here, the SNR penalty denotes the performance gap of the channel with phase noise compared with the pure AWGN channel, given a specific ratio of the linewidth per laser to the symbol rate. It verifies again that the laser linewidth tolerance of star-8QAM is the best, and the tolerance of 16QAM is the worst. 16APSK(8,8) performs slightly better than 16PSK, but worse than 8PSK. More specifically, by considering 1 dB SNR penalty at the BER of 10^{-2}, the maximum tolerable ΔvT of 8PSK is above 10^{-3}, while that of 16QAM, 16PSK and 16APSK are 4×10^{-5}, 9×10^{-5} and 3×10^{-4}, respectively. Additionally, though the slow increase in SNR penalty restricts the maximum tolerance of Star-8QAM from appearing in Fig. 4, the maximum tolerable ΔvT is around 4.5×10^{-3}.

C. Performance Comparison With DA ML PE

It is well known that a large laser linewidth results in a large phase noise variance which will cause a rapidly changing
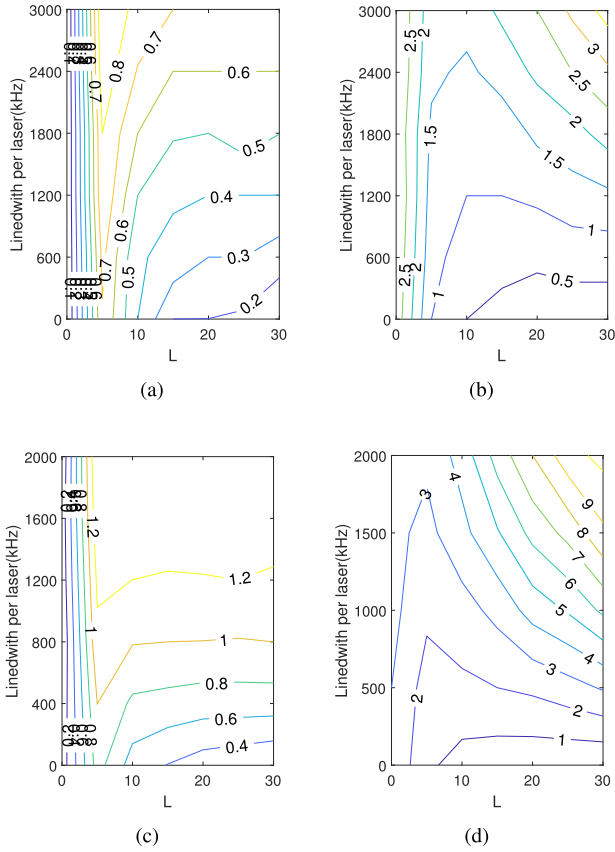
Fig. 5. Receiver sensitivity penalties (dB) at BER=10^{-2} versus the linewidth per laser and memory length L: (a) 8PSK with LMMSE-Es, (b) 8PSK with DA ML, (c) 16PSK with LMMSE-Es, and (d) 16PSK with DA ML.

Fig. 6. Receiver sensitivity penalties (dB) at BER=10^{-2} versus the linewidth per laser and memory length L for (a) star-8QAM with LMMSE-Es and (b) star-8QAM with DA ML.

Fig. 7. Receiver sensitivity penalties (dB) at BER=10^{-2} versus the linewidth per laser and memory length L for (a) 16APSK(8,8) with LMMSE, (b) 16APSK(8,8) with DA ML, and (c) 16APSK(8,8) with LMMSE-Es.

interference to the phase estimation. Therefore, the linewidth tolerance analysis for phase estimation is very important. Moreover, the selection of the memory length L will affect the estimation accuracy in the most existing PE algorithms, which is known as the block length effect. Thus, to test the laser linewidth tolerance of the refined estimators, some numerical comparisons with the popular DA ML PE are performed here. Specifically, the contour plots of the receiver sensitivity penalties for different modulation formats with various linewidths and memory lengths at BER=10^{-2} are shown in detail in Figs. 5, 6 and 7, at a bit rate of 40 Gb/s.

Fig. 5 shows the performance comparison between the average-energy based LMMSE estimator and the DA ML estimator in [14] for single-ring 8PSK and 16PSK. Note that for single-ring PSK, the ring-detection based estimator is equivalent to the average-energy based one. It is shown that given the same linewidth, the SNR penalty of the refined LMMSE estimator is much smaller than that of the DA ML estimator. For example, given the linewidth to be 2.4 MHz for 8PSK, the SNR penalty is 0.6 dB for the LMMSE estimator, whereas it is at least 1.5 dB for the DA ML estimator as shown in Fig. 5(a) and (b). With the continuous increase of L, the receiver sensitivity penalty tends to be stable for the LMMSE estimator, whereas the penalty of the DA ML estimator has a contour growth given a fixed linewidth. Obviously, the DAML method has an optimal memory length L
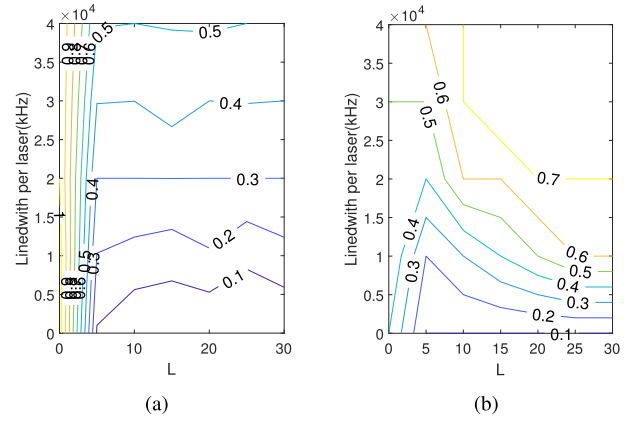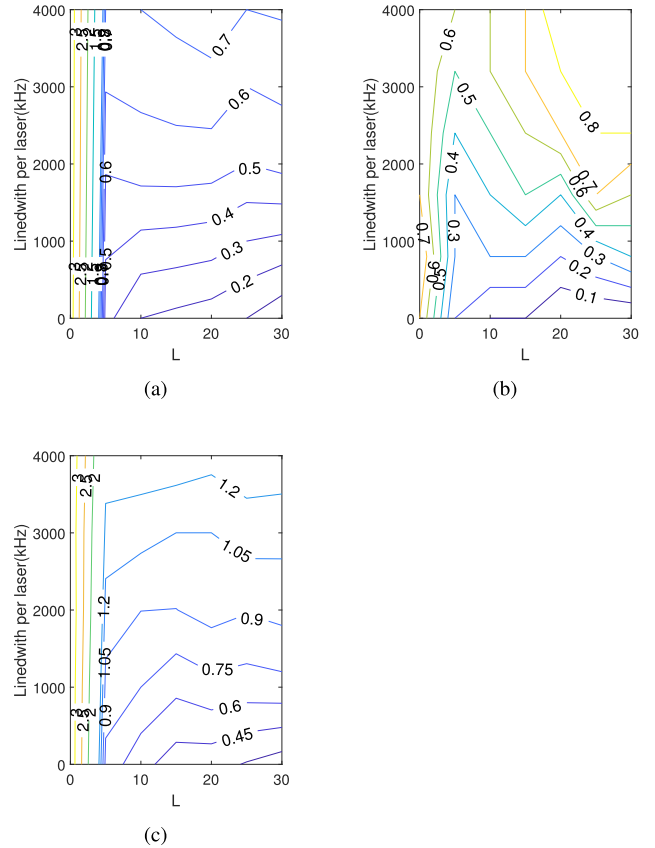
to determine for a given laser linewidth, that is, its performance is affected by the block length effect. In contrast, this proposed method does not suffer from the block length effect. Fig. 5(c) and (d) verify again that even with the simplified implementation, the laser linewidth tolerance of the average-energy based LMMSE estimator remains much better and avoids the block length effect for high-order PSK.

Figs. [6] and [7] show the receiver sensitivity comparison for multi-ring star-8QAM and 16APSK(8,8), respectively. It is worth noting that for star-8QAM, the SNR penalty of the common refined estimator is always about 0 dB throughout the linewidth range considered, which means that it can perfectly compensate the phase and achieve the performance as in pure AWGN. Besides, as can be seen in Fig. [6], the average-energy based method performs better than the DA ML method. When the laser linewidth is set to be 30 MHz, the SNR penalties are about 0.4 dB for the LMMSE estimator and 0.5 dB for the DA ML estimator with the optimal length chosen, respectively. This implies that even the simplified estimator has a better laser linewidth tolerance, compared to the DA ML method which yet requires an optimal L. For 16APSK(8,8) shown in Fig. [7], the laser linewidth tolerance of the common refined estimator and the DA ML estimator are comparable. For example, given the linewidth to be 2 MHz, the SNR penalty is about 0.5 dB for the LMMSE estimator, whereas it is also about 0.5 dB for the DA ML estimator with the optimal length chosen. Whereas, the SNR penalty of the average-energy based estimator is more than 0.8 dB as shown in Fig. [7(c)]. It is worth emphasizing again that the refined LMMSE estimators proposed for multi-ring APSK do not suffer from the block length effect, compared to the popular DA ML method.

D. Performance Comparison With QPSK Partitioning Method

Here, in order to verify the generalization of the refined LMMSE PE method, the well-known QPSK partitioning scheme in [16] is also considered for 16QAM as a comparison. Fig. [8] shows the receiver sensitivity penalty comparison with the QPSK partitioning method for 16QAM. In QPSK partitioning scheme, the received signals are partitioned into two sets during estimation: the signals to be rotated and the benchmark signals (i.e., the signals on the diagonal). Since the rotation is first implemented with reference to the benchmark signals, a limited number of reference points will have a significant impact on the estimation accuracy. Therefore, the memory length L required for QPSK partitioning scheme to achieve BER $= 10^{-2}$ cannot be less than 5, as shown in Fig. [8(b)]. Given the linewidth to be 2.5 MHz, the SNR penalty is 2.5 dB for the QPSK partitioning estimator. And with the continuous increase of L, the SNR penalty exhibits a contour growth. On the contrary, the LMMSE estimator exhibits a superior SNR gain of approximately 1.4 dB with $L = 5$ as shown in Fig. [8(a)], compared to the QPSK partitioning estimator. Additionally, the average-energy based estimator has a slightly worse performance, but will not worsen as L increases. That verifies that our refined LMMSE estimators can be generalized to 16QAM, and the choice of $L = 5$ is more suitable for multi-ring modulated systems with high latency requirement.

E. Complexity Analysis

To indicate the effectiveness of the proposed ring-detection based and average-energy based estimators, in this subsection, we investigate time complexity and computational complexity analysis. As can be observed, the phase estimates of common
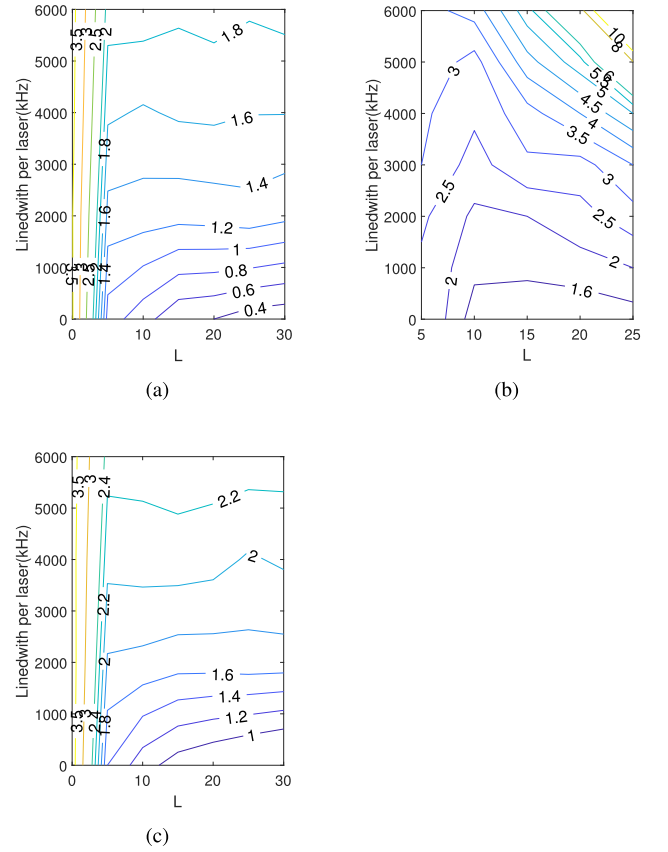

Fig. 8. Receiver sensitivity penalties (dB) at BER$=10^{-2}$ versus the linewidth per laser and memory length L for (a) 16QAM with LMMSE, (b) 16QAM with QPSK partitioning, and (c) 16QAM with LMMSE-Es. Bit rate at 40 Gb/s.

refined LMMSE, ring-detection based and average-energy based estimators are all based on (3). Therefore, here we consider the time complexity involved by (4), (5) and (6). Denote the window length $2L + 1$ as W, then we have the time complexity involved for calculating $\mathbf{R}$ and $\mathbf{p}$ is $O(W^2)$ and $O(W)$, respectively. The complexity for obtaining (4) is $O(W^3 + W^2)$. Suppose the length of entire signal is N_d, the window needs to be updated for $(N_d - 2L)$ times. Therefore, we can obtain that the time complexity of common refined LMMSE estimator and ring-detection based estimator are both $O(W^3(N_d - 2L))$. For the average-energy based estimator, the AOPN variance σ_ϵ^2 is calculated in advance based on SNR, and it is a constant over the entire phase estimation process. Therefore, its time complexity is just $O(W^3)$, which is much lower than that of common refined LMMSE and ring-detection based estimators.

Additionally, for the computational complexity, since the main difference between the common refined LMMSE and ring-detection based estimators is the calculation of AOPN variance, here we just compare the number of real/complex multiplications in (7) and (9), within a single window. It is obvious that for each time index, there are 3 multiplications involved for obtaining $\sigma_\epsilon^2(k)$, which results in $3W$ multiplications in the common refined LMMSE estimator. In (9), the ring-detection

based estimator replaces the time-varying denominator by a constant, resulting in merely 3 multiplications, which is much lower than that of the common refined LMMSE estimator.

In comparison with the DA ML estimator, it is obvious that the DA ML estimator possesses much lower complexity, which is $O(W)$ in one estimation window. However, given the values of SNR, window length W, the phase noise variance σ_p^2, the matrix $\mathbf{R}$ and vector $\mathbf{p}$ actually can be obtained in advance for the weight calculation, i.e., before performing the phase estimation with the proposed average-energy based estimator. Thus, considering the similar implementations of (3) for both methods, the time complexity of the average-energy based estimator can be reduced to merely $O(W(N_d - 2L))$, which is the same as that of the DA ML estimator.

V. CONCLUSION

In this paper, the common refined LMMSE PE method and two simple implementations are proposed for multi-ring APSK and even QAM with Wiener phase noise. The laser linewidth tolerance analysis is provided comprehensively. The numerical results show that the common LMMSE estimator performs much better than the DA ML and QPSK partitioning methods with the optimal length chosen for the latter two. And even the simplified ones do not suffer from the block length effect. The improved receiver sensitivity without sacrificing the complexity enables the proposed estimators to be implemented in a practical multi-ring coherent receiver in high SNR or rapidly-changing phase noise environment.

REFERENCES

[1] N. Shibata, N. Iiyama, J. ichi Kani, S.-Y. Kim, J. Terada, and N. Yoshimoto, "Star-QAM constellation design for hierarchically modulated PON systems with 20-Gbps PSK and 10-Gbps OOK signals," *J. Lightw. Technol.*, vol. 32, no. 18, pp. 3184–3191, Sep. 2014.

[2] H. Kishikawa, M. Uetai, and N. Goto, "All-optical modulation format conversion between OOK, QPSK, and 8QAM," *J. Lightw. Technol.*, vol. 37, no. 16, pp. 3925–3931, Aug. 2019.

[3] A. Soleimanzade and M. Ardakani, "EGN-based optimization of the APSK constellations for the non-linear fiber channel based on the symbol-wise mutual information," *J. Lightw. Technol.*, vol. 40, no. 7, pp. 1937–1952, Apr. 2022.

[4] Q. Wang, Z. Quan, T. Song, M.-W. Wu, Y. Li, and P.-Y. Kam, "M-APSK constellation optimization in the presence of phase reference error," *IEEE Wirel. Commun. Le.*, vol. 9, no. 12, pp. 2154–2158, Dec. 2020.

[5] D. Villafani, J. Schröder, M. Karlsson, P. A. Andrekson, and E. Goobar, "Impact of low frequency laser phase noise in high order modulation formats," in *Proc. SBMO/IEEE MTT-S Int. Microw. Optoelectron. Conf. (IMOC)*, 2019, pp. 1–3.

[6] M. Al-Qadi, M. O'Sullivan, C. Xie, and R. Hui, "Phase noise measurements and performance of lasers with non-white FM noise for use in digital coherent optical systems," *J. Lightw. Technol.*, vol. 38, no. 6, pp. 1157–1167, Mar. 2020.

[7] T. Sasai, A. Matsushita, M. Nakamura, S. Okamoto, F. Hamaoka, and Y. Kisaka, "Laser phase noise tolerance of uniform and probabilistically shaped QAM signals for high spectral efficiency systems," *J. Lightw. Technol.*, vol. 38, no. 2, pp. 439–446, Jan. 2020.

[8] J. Lu et al., "Carrier phase recovery for set-partitioning QAM formats," *J. Lightw. Technol.*, vol. 36, no. 18, pp. 4129–4137, Sep. 2018.

[9] Q. Wang and P.-Y. Kam, "Optimum detection of two-dimensional carrier modulations with linear phase noise using received amplitude and phase information and performance analysis," *J. Lightw. Technol.*, vol. 34, no. 10, pp. 2439–2451, May 2016.

[10] Q. Wang, Z. Quan, S. Bi, and P.-Y. Kam, "Joint ML/MAP estimation of the frequency and phase of a single sinusoid with Wiener carrier phase noise," *IEEE T. Signal Proces.*, vol. 70, pp. 337–350, 2022.

[11] Y. Guo et al., "Phase noise estimation in coherent optical communication based on local convex optimization," in *Proc. IEEE 16th Int. Conf. Opt. Commun. Netw.*, 2017, pp. 1–3.

[12] N. Xie, L. Ou-Yang, and A. X. Liu, "A machine learning approach to phase reference estimation with noise," *IEEE T. Commun.*, vol. 68, no. 4, pp. 2579–2592, Apr. 2020.

[13] Y. Li, M.-W. Wu, X. Du, T. Song, and P.-Y. Kam, "A refinement to the Viterbi-Viterbi carrier phase estimator and an extension to the case with a Wiener carrier phase process," *IEEE Access*, vol. 7, pp. 78170–78184, 2019.

[14] S. Zhang, P. Y. Kam, C. Yu, and J. Chen, "Laser linewidth tolerance of decision-aided maximum likelihood phase estimation in coherent optical *M*-ary PSK and QAM systems," *IEEE Photonic. Tech. L.*, vol. 21, no. 15, pp. 1075–1077, Aug. 2009.

[15] P. Y. Kam, "Maximum likelihood carrier phase recovery for linear suppressed-carrier digital data modulations," *IEEE Trans. Commun.*, vol. 34, no. 6, pp. 522–527, Jun. 1986.

[16] I. Fatadin, D. Ives, and S. J. Savory, "Laser linewidth tolerance for 16-QAM coherent optical systems using QPSK partitioning," *IEEE Photonic. Tech. L.*, vol. 22, no. 9, pp. 631–633, May 2010.